Journal of Visualization, Vol. 5, No. 3 (2002) 233-241

Application of Three-component PIV to the Measurement of Hypervelocity Impact Ejecta

Heineck, J. T.*1, Schultz, P. H.*2 and Anderson, J. L. B.*2

*1 Experimental Physics Group, Aerospace Projects Division, NASA Ames Research Center, Moffett Field, CA 94035, USA.
*2 Department of Geological Sciences, Brown University, Providence, RI 02912, USA.

Received 15 November 2001.
Revised 9 March 2002.

***Abstract*:** Three-component Particle Image Velocimetry has been applied to the measurement of hypervelocity ejecta from meteoritic impact experiments. This work represents the first attempt at measuring ejecta from a ballistic event using the PIV technique. The ejecta particles are measured directly, within a plane, at any controlled instant after the impact. The particle trajectories are observed at all azimuthal positions relative to the impact point thus revealing both the shape of the curtain and the distribution of velocities at a given instance. By seeding the target with 10 μm hollow spheres, the fluid flow associated with the impact in an atmosphere is simultaneously observed with the ejecta. 3C PIV is demonstrated to be an ideally suited technique for investigations on ejecta trajectories, ejecta curtain morphology and the fluid mechanics in the presence of an atmosphere. Sample results are presented.

***Keywords*:** hypervelocity impacts, PIV, ballistic ejecta, meteor impact, Ames Vertical Gun Range.

1. Introduction

Hypervelocity impacts have been investigated experimentally using powder and light-gas guns for forty years at NASA Ames Research Center. Development of new experimental methods, coupled with new perspectives over this time, has greatly improved the understanding of the basic physics and phenomenology of the impact process. The Ames Vertical Gun Range (AVGR) was first developed as part of a series of ballistic ranges to support the Apollo program. Since 1979, the AVGR has operated as a national facility. Fundamental discoveries made at the AVGR have led to novel methods for characterizing the impact cratering process on Earth and on other solar system bodies including the Moon, Mars, Venus and asteroids. The AVGR also has played a key role in defining and supporting numerous NASA missions and mission science including Apollo, Mariner 10, Viking, Magellan, Stardust and the upcoming Deep Impact Mission.

Recently, 3C PIV has been used at the AVGR to investigate the cratering flow field as expressed by its ejecta (Schultz et al., 2000; Anderson et al., 2000). Although PIV can be applied in gun ranges where the projectile is launched horizontally, it is exceptionally well suited for use in the AVGR. The size of the chamber allows tracing ejecta without interference of the walls. Additionally, this facility keeps the target horizontal while elevating the launch tube assembly from angles ranging from vertical to 15° above horizontal. This variable launch angle allows the use of gravity-sensitive targets, such as sand and water. Since the most likely angle of impact is 45° above horizontal (Shoemaker, 1962), this variable angle capability is critical for understanding planetary impact processes (Gault and Wedekind, 1978).

Hypervelocity impacts (not to be confused with hypersonic flow) are defined by the ratio of the impactor velocity and the speed of sound of the target material. If the impactor is traveling faster than the target's sound

speed, it is considered a hypervelocity impact. Aluminum, for example, has a sound speed of approximately 5.5 km/sec, whereas bulk sand has a sound speed typically less than 0.2 km/sec. An impact into sand creates a shock that induces outward particle motions. The rarefaction wave behind this shock is produced by the free surface and redirects these particle motions upward and outward. This redirected flow field forms a stream of particles whose combined positions above the target surface at any given moment in time resemble an inverted cone. Even after the crater has stopped growing, the conical curtain of ejecta expands and marches outward across the surface (Gault et al., 1968). When an atmosphere is present, the characteristics of the ejecta plume change radically. Aerodynamic forces alter the trajectories and distort the curtain. The motion of the curtain through the atmosphere induces two ring vortices, one inside and one outside the curtain, that modify the emplacement of the ejecta (Schultz, 1992a; Barnouin-Jha and Schultz, 1996). Furthermore, the wake of the impactor interacts with both the ejecta and the vortex inside the curtain.

Previous studies of crater ejecta relied on high-speed films, which provided only limited data on the three-dimensional flow field and conditions inside the ejecta curtain. Dust can severely occlude the view of the interior portion of the impact region. Atmospheric disturbances created by an impact are typically invisible to the film record. Experiments have been performed where a plate covers one-half of the crater field and blocks the ejecta curtain (also known as a quarter-space experiment). This experimental design permits the vertical cross-section to be viewed, but not the horizontal cross-section. Cintala et al. (1999) used a particle tracking technique with success, but it was limited to two-dimensional data in only one azimuthal direction around the impact point.

The 3C PIV system meets such challenges. Measurements of a horizontal cross-section of the ejecta plume permit simultaneous assessment of both the ejecta curtain and the dust-carrying flow field. Thus, the occluding dust becomes measurable tracer particles. This view and the data it produces have been unobtainable with other measurement systems. The intent of these experiments is to develop the use of 3C PIV as a robust technique to observe and measure the particle velocities, the fluid dynamics (in the presence of an atmosphere), and observe the curtain morphology for a wide range of impact conditions. A well-developed system can be used for future planetary studies, defining future space missions and test computational models. This report describes the AVGR facility, reviews the PIV system, addresses the timing issues, shows sample data and describes on-going applications.

2. Experimental Design

2.1 Facility Description

The AVGR permits the launching of projectiles, up to 6.35 mm (0.25 inches) in diameter, at multiple angles relative to the target material. With several gun types, the facility can provide launch velocities ranging from 30 m/s to 7000 m/s with launch angles from 15° to 90° in 15° increments. The velocity of the projectile is measured using three shadowgraph stations mounted in the launch tube. These stations use photodetectors to sense the passage of the projectile and produce trigger signals that can be used to synchronize other data acquisition systems to the impact event.

The target resides in a vacuum chamber, (blue tank in Fig. 1(a)) which allows for the simulation of impacts in a wide range of environments. The chamber, about 2.5 m in diameter and 3 m in height, can be evacuated to simulate a celestial body without an atmosphere or can be back-filled with gases that are either inert or can replicate known compositions of atmospheres on other solar system bodies. Target materials can be anything: from ice to water, metal plates, bulk sand and meteorites. Porous sand has been used for several decades in order to understand gravity-controlled crater excavation and therefore there exists a large database for comparison. Containers of sand, each of different fineness, were used for these experiments. A sample of all data will be discussed in following sections.

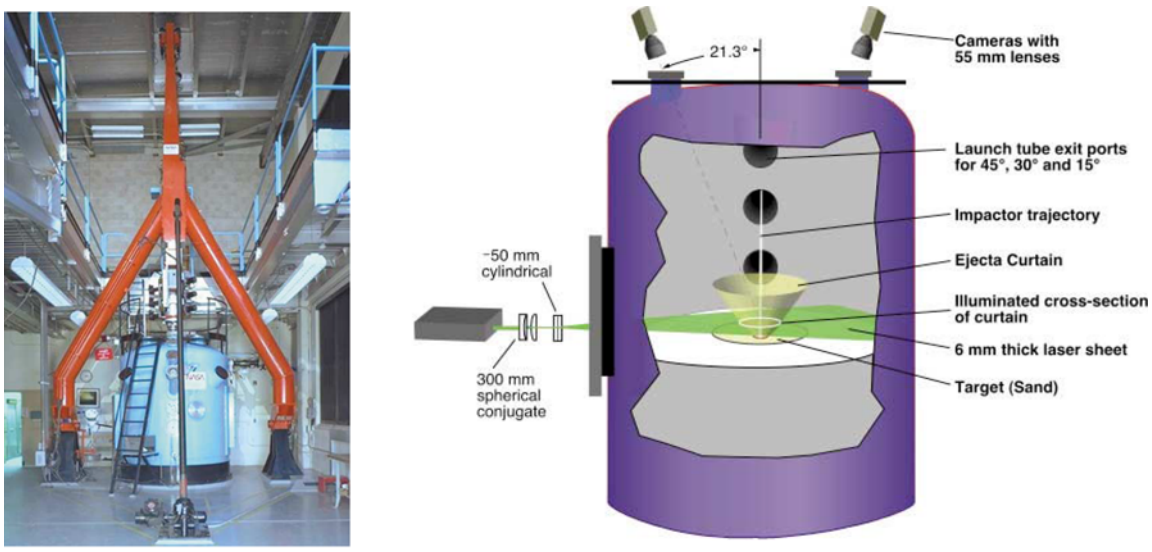

Fig. 1. (a) Photo of AVGR with launch tube at 90° to target. (b) Illustration of PIV system relative to the ballistic chamber (opposite side from photo view).

2.2 The PIV System

The vacuum chamber has several windows suitable for both laser projection and camera viewing. The view required for measuring both the ejecta curtain and the fluid physics was from above the target. Furthermore, this view permitted the observation of asymmetry of the curtain from an oblique impact and tracking of the entire evolution of the curtain. By projecting the laser light sheet from the side, parallel to the target, the circumference of the ejecta curtain was illuminated, as shown in Fig. 1(b).

The 3C PIV system consisted of two Kodak ES 1.0 cameras mounted on Newport motorized translation and rotation stages to remotely apply Scheimpflug focusing of the cameras. The camera sensors are 1008 × 1018 pixels, with 9 μm square pixels. With 55 mm lenses, the field of view covered approximately 40 × 38.5 cm. The pixel resolution was approximately 0.4 mm in object space. The laser was a New Wave Gemini series dual-pulse Nd:YAG with an output of 120 mJ/pulse at 532 nm. The laser plane was established at 89 mm (3.5 inches) above and parallel to the horizontal target and the sheet thickness was optically thinned to 6.35 mm (0.25 inches) using a conjugate set of 300 mm spherical lenses. Interference filters centered on 532 nm were placed between the lenses and the sensors. Laser and camera timing was controlled using a National Instruments 6602 timing board. The timing signals and image recording were controlled through Integrated Design Tool's (IDT) proVISION software (the same software package used to process the image data) and PIV controller unit. This unit contains the timing board and frame grabbers.

The proVISION software includes several features of specific value for these experiments. First is the ability to trigger the cameras and the laser from a single external pulse. Also, a feature in the correlation algorithm simplified the processing. During the error-checking portion of the cross-correlation algorithm, a null value is assigned to grid points where no particle images are present (Lourenco, 2000). This permits the use of a single mesh to cover the entire image of the ejecta curtain. Without that feature, a series of small meshes must be created to cover only the ejecta, which becomes very cumbersome. The data presented below were processed using 24 × 24 pixel interrogation areas, with average particle displacements three pixels or longer. The mode of processing required no less than 10 particle pairs to contribute to the correlation thus meeting the high-density seeding (Lourenco and Krothapalli, 2000). Each sand particle image occupied no less than 3 pixels, whereas the images of pulverized dust trailing the impactor averaged between 2 and 3 pixels. The shortest inter-pulse delay time for the system was 1 μsec. With the sheet thickness of 6 mm, an ejecta particle can travel 1.5 mm vertically inside the sheet (and be detected in both images). Assuming a 45° trajectory, the total travel of the particle is approximately 2.1 mm. A particle moving 2.1 mm in μs (microseconds) converts to 2.1 km/sec. This velocity corresponds to the fastest ejecta and the velocity of surviving impactor material for an initial impactor velocity of 6 km/sec. Thus the system was fully capable of measuring the ejecta velocity of any impact experiment performed at the AVGR.

The PIV system was calibrated according to the dictates of the IDT software. The calibration target was

designed to provide the necessary coordinate points that the software uses to generate the photogrammetic parameters to reconstruct the third component of velocity (Lourenco, 2000). A displacement test using a plate, painted to simulate particle images, was performed in-situ to test the accuracy of the system. This test confirmed the stated accuracy claim of the software to have a maximum error of 2% for in-plane motion and 4% out-of-plane motion.

2.3 Timing Issues

The ejecta velocities decrease as a power law with the stage in crater growth (Schultz and Gault, 1979; Housen et al., 1983). Since the most common technique to date for determining ejecta velocities has been the use of high-speed motion picture, whether or not a cinematic PIV approach is feasible needs to be determined. The advantage of such an approach is clear: more data per impact. However, if the decreasing velocities over time are so great that a single inter-pulse delay time would not adequately measure the spectrum of velocities, then the single-measurement-per-impact approach may be necessary.

For the purpose of this discussion, the evolution of ejecta from an impact can be divided into three stages. The first is from the moment of first contact to the moment of complete energy coupling. With higher velocity impacts, melting and vaporization of the impactor and target may occur, as well as compression in porous materials. During oblique impacts, a plasma jet typically develops with downrange velocities exceeding three times the impactor velocity (Schultz, 1996). This stage lasts less than 10 μs (microseconds) to 50 μs, depending on the velocity of the impactor. The ejecta from this early age are out of the camera's field of view in less than 20 μs to 100 μs.

The second stage of the ejection process is from the moment of complete energy coupling to the end of the crater formation. This lasts about 100 ms (milliseconds) for a 1 km/sec impactor in a sand target. For a 5 km/sec impactor, this stage increases to 120 ms. During this time, the flow field excavates a growing cavity and the rarefaction wave travels outward and dissipates. The ejecta curtain is constantly fed with new material, though less energetic as time passes. The third stage begins with the end of the crater growth and continues until all the ejecta returns to the surface. This lasts for another 750 ms before the particles hit the walls of the tank. Ejecta trajectories of the second and third stages follow conventional ballistic equations based on the initial velocities and initial angles dictated by the subsurface flow, unless modified by the presence of an atmosphere.

The initial approach to determining the inter-pulse timing was by free-running the PIV system at the maximum rate of 15 Hz to acquire as many instances in the fewest number of experiments as possible. After a few successful acquisitions, enough sample data were collected at each stage of the cratering process. Ejecta velocities were then calculated for the various stages of evolution. This strategy permitted the quick comparison of velocities measured in the early stage with those from the late stage. Subsequently, the inter-pulse timing was adjusted to the specific stage of the impact process. A second objective was met with this first series: the effect of targets of different grain size and the effect of impact angle on the cratering flow field, as expressed by the velocity distribution of ejecta within the curtain.

A number of other issues arose during this evaluation; the most important of which is exposure. The sand particle size (approximately 400 μm) is several orders of magnitude larger than the smoke particles typically used in airflow studies. As a consequence, the laser power requirement for a sand particle is quite small. Closing the lens to f22 was insufficient attenuation to prevent saturation. Reducing the flash lamp power caused the beam divergence to increase, thereby causing the light sheet thickness to increase across the measurement area. Also, from earlier work, the visible light produced by the plasma (also known as the impact flash) was determined to be similar in intensity and spectral content to a photographic flash. The intensity of the flash saturated the CCD. Both problems were easily solved with the use of the interference filters centered on the Nd:YAG 2nd harmonic of 532 nm. The power of the laser in that wavelength was significantly greater than that of the plasma, thus the laser light scattering from the particles was the only light recorded. Additionally, since the filter transmits only 50% of the center wavelength, the use of the filter helped prevent the particle images from saturating the CCD.

Synchronizing the PIV system to the moment of impact was first attempted using the trigger signal from the third shadowgraph station. This signal was routed to a digital signal-delay generator, which was set to trigger the PIV system with a calculated amount of delay. The trigger station that generates this signal was approximately 2.5 m from the target. The impactor velocity was subject to variation due to gun barrel and gunpowder conditions. This variation led to uncertainty between the predicted and actual velocity of the impactor. By having the synchronization signal so far away from the target, any error in the timing calculation is exacerbated by these variations. The true timing of the moment of impact and the image acquisition had to be calculated after each shot.

To achieve greater repeatability, a new synchronization method was designed.

A make/break trigger using aluminum foil was then placed inside the chamber. A rail system aligned with the projectile path permitted the adjustment of the distance from the trigger location and the impact location. The current from a 6 VDC power supply was passed through the foil and sent to the digital delay generator. The digital delay generator was triggered off the drop in voltage upon disruption. The trigger foil was placed 225 μs worth of travel distance away from the target, which corresponds to the delay of the PIV system upon triggering. Adding time to the delay generator controlled the recording moment after the impact. The repeatability of event timing was improved by two orders of magnitude. Figure 2 is a top-view drawing of the AVGR with the PIV system and signal routing. Note in this drawing that the base angle of the camera pair is not perpendicular to the impactor path. This angle has no effect on the data, but the reader should recall this when viewing the raw data images in the following section.

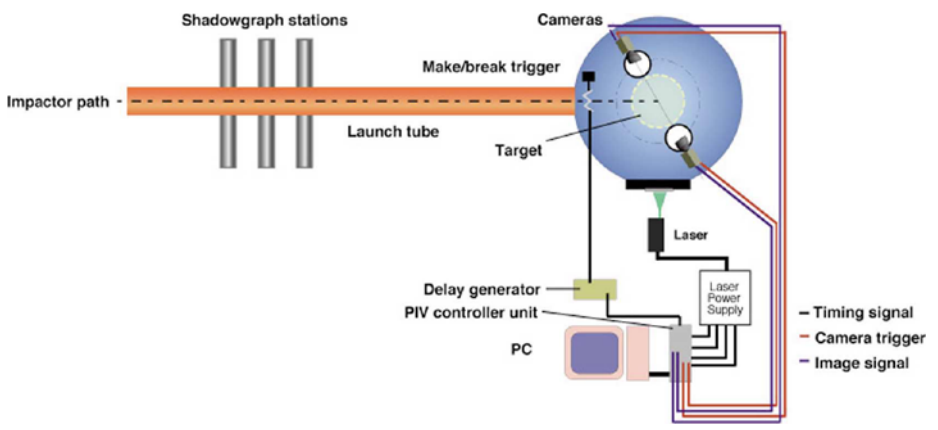

Fig. 2. Top-view illustration of the 3C PIV system and timing signal routing at the AVGR.

3. Results

3.1 Single Impacts: Proof of Concept

As stated above, the initial approach to timing the system to the event was to allow the system to record at 15 Hz for 8 seconds (as limited by RAM) and independent of the firing sequence. Figure 3 is the data set resulting from such a recording. The impactor was 6.35 mm (0.25 inches) Pyrex sphere traveling at approximately 1 km/sec and was recorded approximately 50 ms after impact. The target material was #20 sifted silica sand whose average particle size was approximately 400 μm.

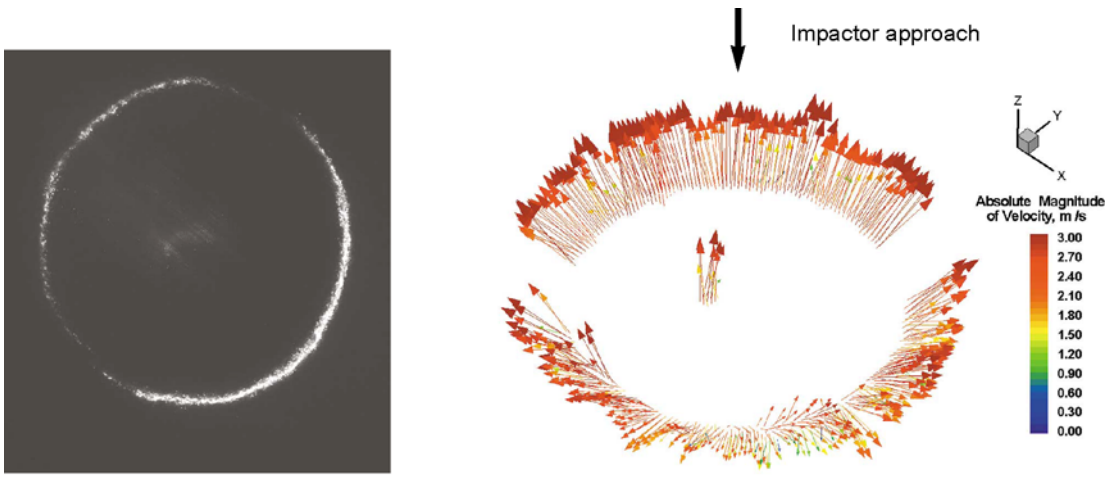

Fig. 3. Data from a vertical impact in a vacuum (a) single image from set (with impactor coming from above) and (b) vector plot of ejecta curtain. Color corresponds to absolute magnitude.

Figure 3(a) is a raw image from the image set. Figure 3(b) shows a vector plot of the impact shown in Fig. 3(a). The discontinuity in the image of the ring in Fig. 3(a) is due to the shadow of the edge of the curtain. The gaps in the data demonstrate the error checking of the software, which renders no data where no particle images exist. Both the curtain's perimeter and the vector angle for the vertical impact show symmetry. The vectors in the center of the ejecta ring represents a reverse plume created by cavitation early in the impact process (Schultz, 1996).

Figure 4 shows the data for an impact made by a 3.25 mm copper sphere traveling at 4.8 km/sec. The target material was the same #20 sand with 10 *m*m microspheres dusting the surface of the sand. The microspheres acted as flow seed. Figure 4(a) is a raw data image of an oblique impact in a nitrogen atmosphere. This impact had enough energy to produce bright plasma; however, use of the 532 nm interference filter successfully prevented contamination of the image. Figures 4(b) and 4(c) are vector plots resulting from the oblique impact, where 4(b) is the top view and 4(c) is the edge view. Note the strong downrange component of flow following the trajectory of the impactor.

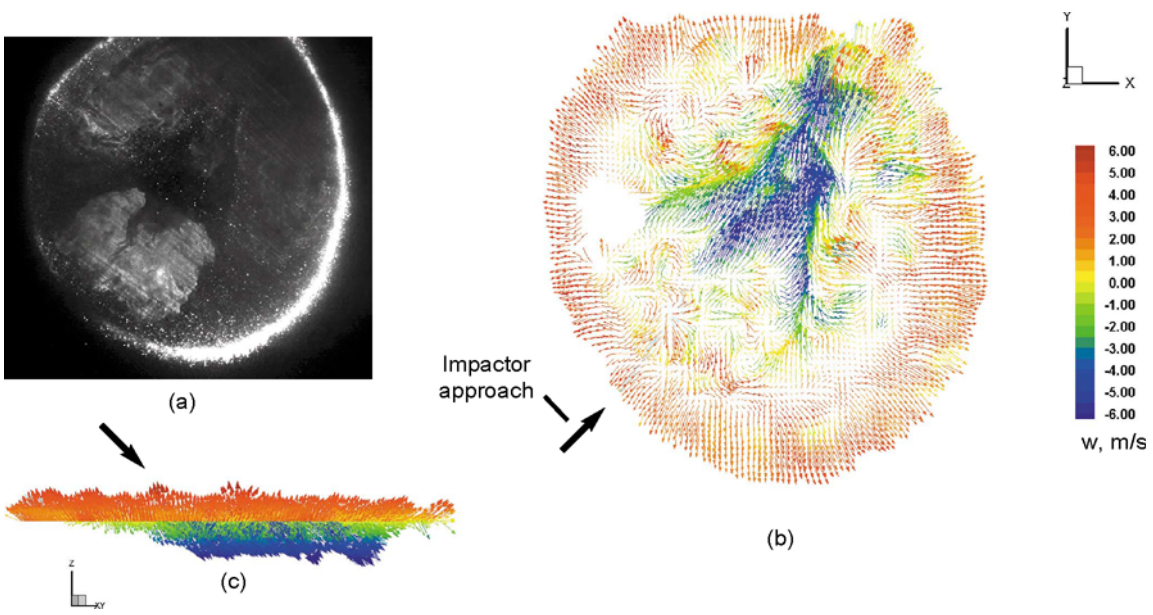

Fig. 4. Data for 45° impact: (a) single raw image from set; (b) top view of vector plot with each vector color representing the vertical velocity component; (c) side view of same data set with vectors colored similarly.

The wake of the impactor and trailing flow of hot gas and debris downrange create a downwash effect long after the impactor itself has disappeared into the target. Evidence for this process can be seen in surface patterns downrange from oblique impacts on Venus where the dense atmosphere enhances the process (Schultz, 1992b). At later times, the ejecta curtain creates a strong ring vortex as it moves outward through the atmosphere. This vortex expands outward along the surface and reworks ejecta deposits to form turbidity flows. This vortex has a strong influence on the pattern of ejecta emplacement including rampart-bordered flows and lobate patterns (Schultz, 1992a; Barnouin-Jha and Schultz, 1996). Also, the ejecta curtain is distorted downrange of the impact site. This distortion is attributed to the early-time ejecta and its wake, whose velocity was roughly one-third that of the impactor. This plot clearly demonstrates the advantages of 3D PIV and its ability to permit visualization and quantification of the complex flow field of the aftermath of an atmospheric impact.

3.2 Shot Sequencing: Spotting Trends

With improved event synchronization and prediction of ejecta velocities, the pulse interval was more accurately tuned for each shot as well. Figure 5 shows sample images from a series of seven matched shots. Each shot was a 30° impact of 6.35 mm Pyrex sphere with a velocity of approximately 1 km/s. The time after impact (t_i) and inter-pulse timing (Dt_p) for each is shown in Fig. 5. Each time-after-impact value was calculated after the true velocity of the impactor was determined.

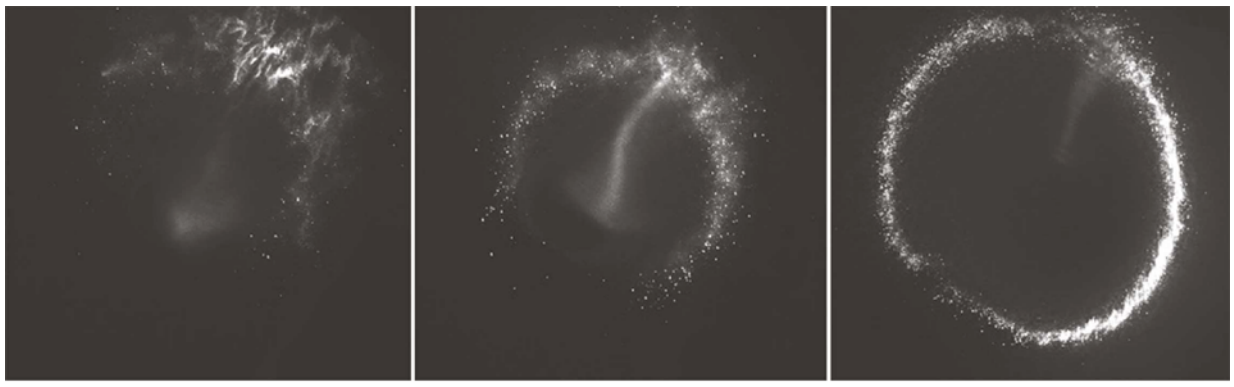

Fig. 5. Samples of raw images, sequenced in time after impact, from 30-degree impact angle series.

Tight control of the synchronization allows for the capturing of each phase of the impact process. At t_i = 1.70 ms, the ejecta from the initial impactor/target interaction pass through the laser plane (recall: 89 mm above the target). The second image shows ejecta above the still-forming crater. The third image shows the curtain while the crater is approximately half-formed and all particles are following ballistic trajectories. The cross-section now shows a complete ring.

Figure 6 shows vector plots, rendered here in a perspective view, resulting from the images in Fig. 5. The vectors for each plot are at the same scale, as is the color scale of absolute magnitude. Note the precipitous drop in velocity from t_i = 1.7 ms to t_i = 7.61 ms. While it is difficult to see in these plots, the velocity drop from t_i = 7.61 to t_i = 49.6 is another order of magnitude. The pulse interval requires adjustment when attempting to optimize the accuracy of the correlation. Also important in this plot is the fact that the spectrum of velocities in each instant are quite narrow, thus the dynamic range of the PIV system was adequate.

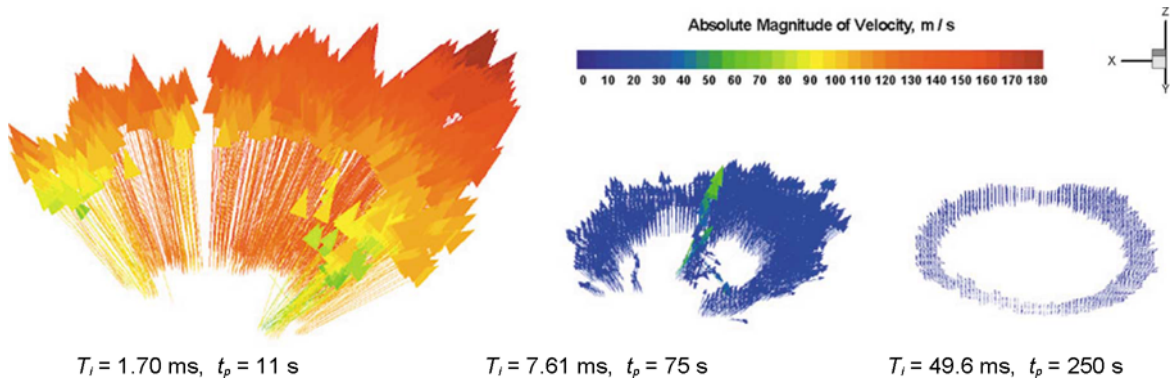

Fig. 6. Oblique views of three-component vector plots of the same sequence. Vector color indicates absolute magnitude of velocity.

The experiment series that resulted in Figs. 5 and 6 are a small sample of the data. By processing all data from the 30° impacts with varying impactor velocities, a statistical base was created. Figure 7 is a plot of the maximum absolute-magnitude velocity observed (V_{Emax}) versus time after impact (T_i) for several 30° impacts. These values are from the first-pass processing and not corrected using the scaling laws (Housen et al., 1983) for the variances from shot to shot. However, the plot demonstrates that the system is measuring the ejecta velocities in accordance with the scaling laws.

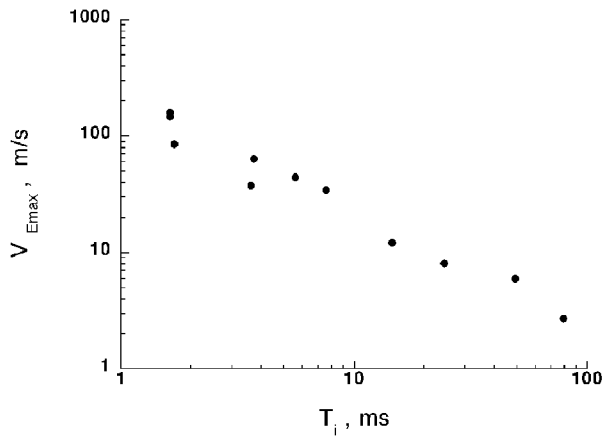

Fig. 7. Plot of maximum ejecta velocity (V_{Emax}) vs. time after impact (T_i) derived from the 30° impact series depicted above.

This plot is intended to demonstrate the level of shot-to-shot repeatability and thus the predictability of the ejecta velocities of a given experiment. This predictable velocity greatly reduces uncertainty in the calculation of the inter-pulse delay required for a given impactor velocity and t_i. Despite the varying shot parameters, the relationship remains logarithmic in scale. Different pulse intervals are required for the different stages of the impact process. Since the velocities of the ejecta slow logarithmically with time, the pulse interval must increase logarithmically. This suggests that a cinematic PIV approach to record a single impact event through its history does not seem feasible without the use of several systems

4. Conclusion

3C PIV has been successfully applied to the measurement of hypervelocity impact ejecta. Synchronization of the event is necessary to optimize the pulse interval time to the age of the impact processes. The dynamic range of the measurement system encompasses the spectrum of velocities observed at a given instance. However, a single pulse interval value is not adequate for the spectrum of velocities through the history of a given impact event. Since the ejecta velocities decrease logarithmically with time, a cinematic PIV approach to a single shot is not advisable at this time. This early success shows that 3C PIV is an excellent tool for the detailed study of these and other ballistic events.

Ongoing research will exploit this new technique. Characterization of ejecta velocities and angles from oblique impacts will continue. Capturing the early-stage flow field created by oblique impacts will contribute to the current interest in meteorite survivability: a key subject for astrobiologists. Documenting vortex generation and evolution created by an impact will contribute to the understanding of ejecta emplacement and therefore studies of craters on the earth and other planets. Assessing the effect of target properties on the ejecta is important for understanding the nature of surface materials on planets, asteroids and comets. These studies support not only basic research, but also planning for the 2005 Deep Impact Mission. This mission will release a 350 kg impactor that will collide with Comet P Temple 1. The onboard instruments will record the formation of the resulting crater, which may be as large as 500 times the size of craters produced by the presented experiments. Results from further 3C PIV measurements of experiments using different target materials and types will provide benchmarks for interpreting the data from this mission.

References

Anderson, J. L. B., Schultz, P. H. and Heineck, J. T., A New View of Ejecta Curtain During Oblique Impacts Using 3D Particle Image Velocimetry, Lunar Planetary Science Conference XXXI, #1794, (Houston, TX, USA), (2000).

Barnouin-Jha, O. and Schultz, P. H., Ejecta Emplacement by Impact Generated Ring Vortices: Theory and Experiments, J. Geophysical Research, 101 (1996), 21 099-21115.

Cintala, M. J., Berthold, L. and Hoerz, F., Ejection Velocities from Impacts into Coarse-grained Sand, J. Meteoritics & Planetary Science, 34 (1999), 605-623.

Gault, D. E., Quaide, W. L. and Oberbeck, V. R., Impact Cratering Mechanics and Structures, in Shock Metamorphism of Natural Materials, (eds. B. M. French and N. M. Short), (1968), 87-99, Mono, Baltimore, USA.

Gault, D. E. and Wedekind, J. A., Experimental Studies of Oblique Impact, Proc. 9th Lunar Planet. Sci. Conf., (1978), 3843-3875.

Housen, K. R., Schmidt, R. M. and Holsapple, K. A., Crater Ejecta Scaling Laws: Fundamental Forms Based on Dimensional Analysis, J. of Geophysical Research, 88 (1983), 2485-2499.

Lourenco, L. M. and Krothapalli, A., TRUE Resolution PIV: A Mesh-free Second Order Accurate Algorithm, International Conference of Lasers to Fluid Mechanics (Lisbon, Portugal), (2000).

Lourenco, L. M., Manual for proVISION Software (2000).

Schultz, P. H., Atmospheric Effects on Ejecta Emplacement, J. Geophysical Research, 97 (1992a), 11623-11662.

Schultz, P. H., Atmospheric Effects on Ejecta Emplacement and Crater Formation on Venus from Magellan, J. Geophysical Research, 97-E10 (1992b), 16183-16248.

Schultz, P. H., Effect of Impact Angle on Vaporization, J. Geophysical Research, 101 (1996), 21117-21136.

Schultz, P. H. and Gault, D. E., Atmospheric Effects on Martian Ejecta Emplacement, J. Geophysical Research, 84 (1979), 7669-7687.

Schultz, P. H. and Gault, D. E., Prolonged Global Catastrophes from Oblique Impacts, in Geological Society of America Special publication 247, (1990), 239-261.

Schultz, P. H., Heineck, J. T. and Anderson, J. L. B., Using 3-D PIV in Laboratory Impact Experiments, Lunar Planetary Science Conference XXXI, #1902, (Houston, TX, USA), (2000).

Shoemaker, E. M., Interpretation of Lunar Craters, in Physics and Astronomy of the Moon, (ed. Z. Kopal), (1962), 283-359, Academic Press, New York, USA.

Author Profile

James T Heineck: He received his BA in Scientific Photography and Color Technology from Brooks Institute of Photographic Arts and Sciences, Santa Barbara, CA in 1987. In 1990, he began work as a scientific and technical photographer at Ames, during which he was granted a patent and earned an Ames Honor Award for Excellence in Technical Service. Since 1998, he has been developing applications for 3C PIV for use in wind tunnel environments ranging from truck aerodynamics, rotor blade vortex measurements in both hover and forward flight and US Navy ship airwake characterization, in addition to the work presented here. Other research interests include flow visualization of full-scale aircraft, schlieren techniques and high-speed PIV.

Peter H. Schultz: He is a Professor of Geological Sciences at Brown University in Providence Rhode Island. He received his Ph.D. in Astronomy from the University of Texas at Austin in 1972. He was a Senior Staff Scientist at the Lunar and Planetary Institute prior to moving to Brown in 1984. He is currently the Science Coordinator for the NASA Ames Vertical Gun Range, Director of the Rhode Island Space Grant and Director of the Northeast planetary Data Center. His research focuses on planetary impact cratering using hypervelocity impact experiments as a means to constrain and test both observational data from various planetary missions, theoretical models and geological field studies. He was a member of the Magellan mission to Venus and is currently a Co-Investigator on NASA's Deep Impact Mission to a comet in 2005. His current research includes: formation and evolution of planetary impact craters, atmospheric effects on ejecta emplacement, oblique impact processes and cratering mechanics in different target materials.

Jennifer L. B. Anderson: She is a Ph.D. candidate in the department of Geological Sciences at Brown University in Providence, RI, from which she received her MSc degree in 2001. She is a National Science Foundation Graduate Research Fellow and a NASA Space Grant Fellow. She completed her bachelors degree in Geophysics, Astrophysics and Physics at the University of Minnesota, completing her BS degrees in 1998. Her research interests include: experimental impact cratering, ejecta mechanics, cratering flow field evolution and the dependence of the cratering process on target material properties.